A Coolant-Free Generic Replacement for a Reactor Cavity Cooling System: Steady-State Normal Operation Analysis of Implementation for a Sodium-Cooled Fast Reactor

Andrew R Gironda,[a] Abderrafi M. Ougouag,[b] R. Sonat Sen,[b,c] Farzad Rahnema,[a] George W. Griffith,[b] and Dingkang Zhang[a]

[a] Georgia Institute of Technology
770 State St NW, Atlanta, Georgia, USA

[b] Idaho National Laboratory
MS3860, 2525 N. Fremont Avenue, Idaho Falls, ID 83401

[c] Present affiliation: Valar Atomics (https://www.valaratomics.com)

agironda3@gatech.edu, abderrafi.ougouag@inl.gov, Sonat@valaratomics.com, farzad@gatech.edu, george.griffith@inl.gov, dingkang.zhang@gatech.edu

ABSTRACT

A new device that replaces active Reactor Cavity Cooling Systems (RCCS) is proposed. The device acts as mostly an insulator during normal operations as the bulk of in-core generated heat is evacuated via the normal reactor cooling path into the plant's energy conversion system. When the reactor is shutdown or if normal cooling paths are not available, the device transitions from a heat path into an ultimate heat sink. The device does not use cooling fluids and instead performs its functions via conduction and radiative heat transfer. Passive RCCS designs often rely on continued availability of a coolant fluid and a path for the fluid to ensure natural convection heat transfer to an outside sink. The new device relaxes the need for fluids and thus makes reactor deployment site-neutral (e.g., possible in arid regions). Also, the device does not require the availability of a coolant path. Yet it is passive, needing no external energy supply and no operator intervention.

The Passive Reactor Radiative Thermal Sink (PaRRaTS) system relies on a radiative heat transfer "valve" made of two shells to control the heat flow out of the reactor vessel wall into a surrounding soil heat sink. The inner side of the outer shell of PaRRaTS is fitted with metal fins that extend into the surrounding soil to deposit removed heat. The inner shell is also fitted with fins that interweave between those of the outer shell without contact. Thus, at lower temperatures PaRRaTS is essentially insulating, while at higher inner temperatures net radiative heat transfer from the inner to the outer shell becomes significant. The system is modeled using Idaho National Laboratory site soil and its performance is assessed. Annual fluctuations in soil makeup and temperatures are considered in setting boundary conditions. Another model input includes the variety of material properties for each section of the PaRRaTS device. The materials are selected based on their function within PaRRaTS. The selection optimizes thermal conductivity, specific heat, and emissivity with cost limits as a constraint. The effectiveness of this system is compared to the Reactor Vessel Air Cooling System (RVACS) of a model sodium-cooled fast reactor. The objective is a nearly insulating system under normal operating conditions, removing less heat than RVACS, that reverts to a more conducting one removing more heat following a SCRAM.

Performance is assessed by the maximum temperature of the soil and the radiative heat transfer between the two PaRRaTS shells. A steady state model is used for normal operating conditions, and steady state and initial transient conditions are used and compared for SCRAM. The ABAQUS code is used for the finite-element thermal analysis of PaRRaTS. A Python script facilitates the process. Results show that during normal operations PaRRaTS does not significantly heat up the soil, nor does it remove more heat than traditional RVACS. SCRAM conditions are addressed in a companion paper.

Keywords: *nuclear energy, heat transfer, passive safety, ultimate heat sink, reactor cavity cooling system, reactor vessel auxiliary cooling system, RCCS, RVACS, thermal valve, passive cooling, heat transfer*

1 INTRODUCTION

Since the very early days of nuclear reactor design and construction, going back to the very first controlled nuclear chain with its axe man, safety has been a paramount consideration[1]. Since those early days, safety systems have been improved greatly to keep up with the increasing complexity of nuclear reactors over time. Safety systems may be active or passive. The latter take advantage of natural forces without requiring external power to function [2]. One concern with passive systems is their limited capabilities. Some methods, such as natural circulation, can only remove heat for a limited time before losing effectiveness [2]. Another constraint on such systems is the required continued access to a coolant inventory and/or to a path for a cooling fluid. The object of this paper is to present a new passive system for accommodating decay heat in a shutdown reactor that does not require a coolant nor a path for coolant circulation. The new system is essentially insulating during normal operations when heat from the core is transported via the normal cooling system. It then transitions into a heat path when the normal cooling path is not available, such as in the event of loss of coolant or flow in normal the cooling system. A shutdown cooling system that avoids the requirement of a coolant's path, qualification, and maintenance prescriptions would make the reactor easier to deploy to otherwise difficult to accommodate locations. This would make the power plant "site-neutral" as far as shutdown cooling or emergency core cooling is concerned. Another potential benefit of the proposed system is enhanced thermal inertia, albeit provided outside the reactor vessel rather than within it. Thermal inertia increases the amount of time between reactor shutdown and when external cooling becomes necessary to prevent fuel failure or vessel damage. This safety enhancement would be most obvious in the case of microreactors, which are physically small and do not benefit from the presence of massive reflectors as would be the case in large HTGRs.

In this paper, the steady-state performance of the PaRRaTS system during normal operation is evaluated. A successful system would be one that does not cause excessive energy loss to the environment radially from the reactor vessel, with such losses staying at the same level or lower than corresponding losses via RCCS or RVACS. A companion paper will present a performance analysis of a shutdown reactor where PaRRaTS is handling the decay heat without aid of other safety systems. In that later study, the goal would be to demonstrate that the system is at least as effective as a cooling path as the RCCS or RVACS of common reactor designs.

The reactor design used as basis in this article is a small, modular, metal-fuelled, pool type sodium-cooled fast reactor. The design metrics and thermals of the reactor used as the design bases can be seen in Table 1.

Table 1: Design Metrics for Model Reactor

Parameter	Value
Electrical Output	311 MW
Thermal Output	840 MWt
RPV Height	17.78 m
RPV Diameter	5.74 m
CV Diameter	6.096 m
Primary Sodium Inlet Temperature	360 °C
Primary Sodium Outlet Temperature	499 °C
Primary Sodium Flow Rate	5.1 m^3/s
Reactor Pressure Wall Temperature Top	404 °C
Reactor Pressure Wall Temperature Bottom	316 °C
Containment Wall Temperature Top	227 °C
Containment Wall Temperature Bottom	171 °C

The safety system that is taken for reference is the Reactor Vessel Auxiliary Cooling System (RVACS), which is a passive and/or active safety system used in liquid metal reactors [3]. RVACS is a type of Vessel Cooling System (VCS) where decay heat is removed from the vessel through its walls by way of convection and/or radiation [3]. RVACS can be either a passive or an active system, where the difference is natural versus forced convection.

RVACS can use both convection and radiation to transfer heat from the guard vessel to a finned shell, which is then cooled through natural convection. Fins are attached to the guard vessel and finned shell, which alters the heat flux between the two walls [4]. The finned walls add a layer of resistance between the RPV and convection boundary. The RVACS system has been found to output 0.65 MWt of thermal energy during normal reactor operations [5].

1.1 HEAT TRANSFER

Heat transfer plays a vital role in nuclear power applications because it is the method in which thermal energy is moved away from the reactor to be converted into electrical energy. Heat transfer is the movement of thermal energy due to a temperature difference [6]. All three mechanisms of heat transfer (conduction, convection, and radiation) are present at the ordinary outer boundary of reactor vessels. However, only conduction and radiation are discussed as they are the modes present in the PaRRaTS device.

Conduction is the mechanism whereby heat is transferred across a temperature gradient from a region of high temperature to one of low temperature across a physical, nonmoving medium [6]. The rate at which heat is transmitted or transported, i.e., the heat flux, is proportional to the thermal conductivity of the material, as given by Equation 1.

$$q_C'' = -k\frac{dT}{dl} \tag{1}$$

Thermal radiation is the process whereby heat is emitted by a material that is at a non-zero absolute temperature[6]. This process does not require the presence of a material in the space of transfer, allowing for radiation to occur in a vacuum. Emissivity, ε , is the measure of how efficiently a surface emits energy compared to a blackbody surface, and ranges from 0 to 1 [6]. A blackbody is a surface that has an emissivity of 1. The thermal radiative heat flux between two surfaces, A and B, can be evaluated using Equation 2 below. In this equation A_X is the area of the X surface and V_{XY} is the view factor between surfaces X and Y. The view factor is the fraction of the radiation leaving

surface X that is intercepted by surface Y [6]. This value is determined by the orientation of each surface and the distance between the two surfaces.

$$q''_{AB} = \frac{\sigma(T_A^4 - T_B^4)}{\frac{1-\epsilon_A}{\epsilon_A A_A} + \frac{1-\epsilon_B}{\epsilon_B A_B} + \frac{1}{V_{AB} A_A}} \quad (2)$$

1.2 SOIL TEMPERATURE

The temperature of soil is dependent on a variety of factors, such as the composition, moisture content, depth of the soil, and climate. The temperature fluctuates throughout the day and annually [7]. The annual fluctuation of the daily average soil temperature as a function of day and depth can be found with Equation 3.

$$T(z,t) = T_a + A_0^{-\frac{z}{d}} \sin\left[\frac{2\pi(t-t_0)}{365} - \frac{z}{d} - 0.5\pi\right] \quad (3)$$

In the above, T_a is the average soil temperature, A_0 is the annual amplitude of the temperature of the surface soil, d is the damping depth, and t_0 is the time lag from a specified date. Damping depth can be found with Equation 4, where $D_h$is the thermal diffusivity of the soil [7].

$$d = \sqrt{365 D_h \pi} \quad (4)$$

Equation 3 doesn't account for the moisture content in the soil but still is a good approximation since the prediction is made using measured data from the area [7].

2 METHODOLOGY

The following section covers the logic followed in selecting which materials are used in the design of PaRRaTS. Also discussed are the properties of the selected materials, the boundary condition temperatures, and how the model was created and solved.

2.1 MATERIAL REQUIREMENTS

PaRRaTS is constituted of multiple sections, each serving a different purpose. Figure 1 shows the breakdown of each section. The corresponding model is broken up into conductors, insulators, coatings and fill gas. The main parts of PaRRaTS are the inner shell and the outer shell. Both are conductors that include sub-parts. The thermophysical properties of the various sections are either minimized or maximized based on the purpose of the section. Table 2 shows the desirable thermophysical property trends for each section. The arrows pointing implies the property needs to be minimized.

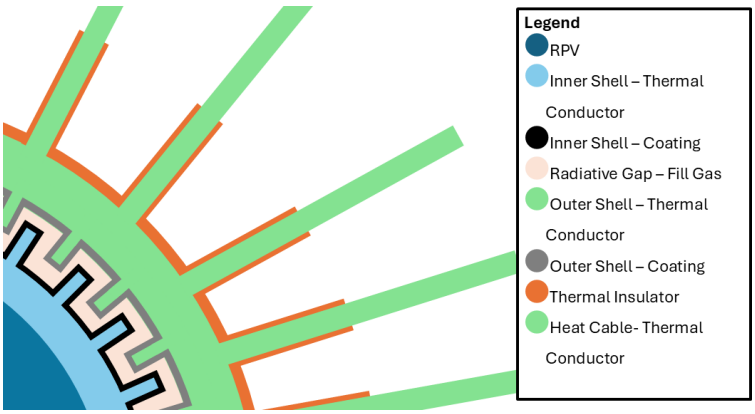

Figure 1: PaRRaTS Cross Section

Table 2: PaRRaTS Sections and Property Maximization/Minimization

Section	Thermal Conductivity	Specific Heat	Emissivity
Conductor	↑	↓	↑
Insulator	↓	↓	↓
Fill Gas	↓	↑	↓
Coating	↑	↓	↑

The steady-state ABAQUS simulation is simplified by modelling only the conducting sections. Insulation will be added later to control the heat flow, and a vacuum is assumed for the radiative section. In the initial model, no coating presence is assumed.

The material for a given section must meet a set of requirements. The first requirement is that the material can support itself. This applies to any solid material used within PaRRaTS, where it should be able to hold itself up and retain its shape without any external support. Euler's buckling formula is used along with the formula for the weight of the object to express property numerically as shown in Equations (5) and (6) [8]. The force in Equation (5) is the critical load that an ideal column can withstand before buckling. The only load in the various elements of PaRRaTS are from their own mass or weight.

$$Force = \frac{\pi^2 EI}{(KH)^2} \tag{5}$$

$$Weight = HAg\rho \tag{6}$$

In these equations, E is Young's modulus for the material, I is the moment of inertia of the cross-sectional area of the structure, K is the column effective length factor (that accounts for the presence of end supports), H is the height of the column, A is the cross-sectional area, g the gravitational acceleration and ρ is the density of the material. Setting these equations equal and solving for H, one gets Equation 7:

$$H = \left(\frac{gA\rho\pi^2 EI}{K^2}\right)^{\frac{1}{3}} \tag{7}$$

The only values that are material specific are the Young's modulus and density, so materials can be compared by those parameters. Figure 2 shows a visual representation for this relation and Equation 7.

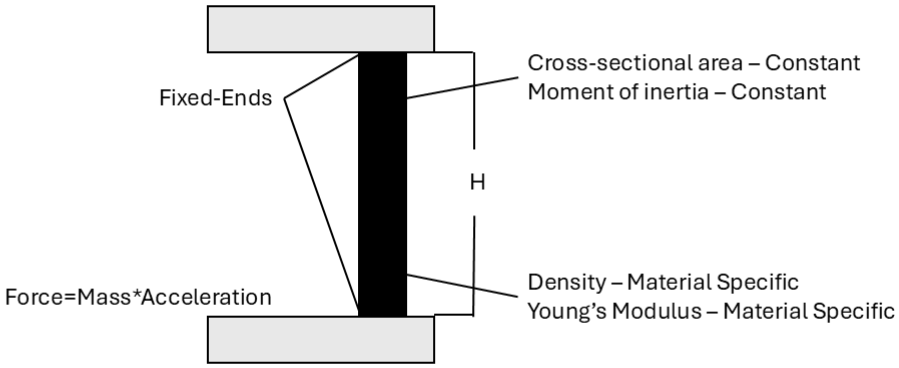

Figure 2: Maximum Height from Critical Buckling Load

The second requirement is that the material must not melt. The temperature limit for a nuclear Reactor Pressure Vessel (RPV) is 700 F per ASME BPVC Section III-1 NCD [9]. Any material that is being used, especially material that is physically closer to the RPV, must have a melting point substantially above this value.

The third requirement is that all materials used in PaRRaTS must be resistant to radiation damage. A device that is either severely damaged before the end of its service life or requires more frequent maintenance than what is scheduled for the nuclear plant would not be useful as a safety system. This requirement is more important for the materials closest to the RPV due to radiation intensity attenuating with distance.

The fourth requirement is the cost of the material. The cost of copper and silicon carbide was selected as the maximum cost per kilogram for reference. This results in the limit being $10 per kilogram [10] [11]. There are some exceptions made for cases where a minimal amount of material is used, such as in the coatings or the restraining band, which is a feature included in the design for holding the inner shell in place against the RPV.

For the inner shell, an additional constraint is for the material in contact with the RPV to be chemically and thermodynamically compatible with that of the RPV. For example, it must not be prone to chemical or physical reactions with the RPV, including not being able to form a eutectic pair that could change melting points. For these reasons, the inner shell must have an innermost portion (referred to as inner-shell-1) made of the same material as the RPV. The outermost portion will be named inner-shell-2 in this article.

2.2 SELECTED MATERIALS

The materials selected for PaRRaTS are steel 316 for inner-shell-1, copper for inner-shell-2 and aluminium for the outer shell. Steel 316 is selected for inner-shell-1 since it acts as a boundary layer between the RPV and rest of PaRRaTS. This is done primarily for chemical compatibility and to prevent eutectic mixing from occurring, which could affect the stability and chemical composition of the RPV steel. Copper is selected for inner-shell-2 since it is exposed to high temperatures. Copper's thermophysical properties make it ideal for heat transfer applications, but its high cost prohibits its use in large applications. Aluminium is selected for the outer shell since it is exposed to lower temperatures than inner-shell-2 makes up a significant portion of the volume of PaRRaTS. Its lower cost when compared to copper makes it better suited for the larger section.

The thermal conductivity, density, specific heat, and emissivity of these materials were gathered to be plugged into ABAQUS as temperature-dependent values. Table 3 shows these values for aluminium, Table 4 shows the values copper, and Table 5 shows the values for steel 316 [12] [13] [14] [15].

Table 3: Aluminium Thermophysical Properties

Thermal Conductivity

Temperature (K)	Thermal Conductivity (W/mK)
273	236
350	240
500	236
700	225
900	210

Specific Heat

Temperature (K)	Specific Heat (J/kgK)
273	881
300	903
500	944
700	1094
900	1194

Density

Temperature (K)	Density (kg/m^3)
200	2719
250	2710
300	2701
400	2681
600	2639

Emittance

Temperature (K)	Emittance
573	0.1
673	0.12
773	0.13
873	0.11

Table 4: Copper Thermophysical Properties

Thermal Conductivity

Temperature (K)	Thermal Conductivity (W/mK)
273	403
350	396
500	386
700	373
1000	352
1360	328

Specific Heat

Temperature (K)	Specific Heat (J/kgK)
280	381
400	398
600	418
800	436
1000	457
1360	492

Density

Temperature (K)	Density (kg/m^3)
300	8930
400	8884
600	8787
800	8642
1000	8568
1200	8458

Emittance

Temperature (K)	Emittance
595	0.493
637	0.496
745	0.539
813	0.589
971	0.769
1040	0.855

Table 5: Steel 316 Thermophysical Properties

Thermal Conductivity

Temperature (K)	Thermal Conductivity (W/mK)
270.00	13.40
482.10	15.10
592.50	18.40
812.60	20.50
953.80	21.80
1220.00	25.10

Specific Heat

Temperature (K)	Specific Heat (J/kgK)
273.00	460.20
373.00	492.50
573.00	536.40
773.00	570.70
1073.00	615.90
1173.00	631.80

Density

Temperature (K)	Density (kg/m^3)
300	7894
600	7783
900	7652
1200	7499
1400	7386
1600	7264

Emittance

Temperature (K)	Emittance
434	0.25
1026	0.34

The soil that surrounds the PaRRaTS device plays a major role as the ultimate heat sink (UHS) into which the removed heat is deposited. The thermophysical properties that need to be known for the soil are the thermal conductivity, specific heat, and the density. The thermal conductivity of soil is a function of its composition, density, and water saturation [16]. The soil composition that is used in the model is that of Idaho National Laboratory's (INL) Critical Infrastructure Test Range Complex (CITRC) facility. It is taken from a report on Soil Activation Model at that facility. Samples were taken across the INL site, where the soil type is determined for different depths. The topsoil layer is primarily clay, followed by basalt and lava layers [17]. Tables 6 and 7 show the thermal conductivity, specific heat, and density over different temperatures for clay and basalt, respectively [12] [18] [19] [20] [21].

Table 6: Clay Thermophysical Properties

Thermal Conductivity

Temperature (K)	Thermal Conductivity (W/mK)
253	2.05
273	1.58
333	1.51

Specific Heat

Temperature (K)	Specific Heat (J/kgK)
273	2.35
300	2.12
350	1.78
400	1.52

Density

Temperature (K)	Density (kg/m^3)
373	1611.2
673	1702.9

Table 7: Basalt Thermophysical Properties

Thermal Conductivity

Temperature (K)	Thermal Conductivity (W/mK)
442.00	1.36
483.00	1.45
529.00	1.53
623.00	1.72
762.00	1.60
858.00	1.63

Specific Heat

Temperature (K)	Specific Heat (J/kgK)
375.0	854.9
536.1	973.0
721.6	1044.6
847.2	1081.6
1004.9	1104.3
1166.8	1142.5

Density

Temperature (K)	Density (kg/m^3)
273	2704.7
1573	2760.4

2.3 BOUNDARY CONDITIONS

Three boundary conditions must be determined and applied to the PaRRaTS thermal model prior to solving it. The first two are the soil boundary conditions, the third is the reactor boundary condition.

The soil instance in ABAQUS is a cylindrical volume where the top layer is assumed to be the temperature varying layer and the bottom layer is assumed to be the constant temperature layer. Clay and basalt are used as soil materials due to the theoretical placement of this device at the INL site. The soil composition used was clay for the first 4.3 meters from the surface, followed by basalt.

The bottom layer is assumed to be part of the constant-temperature layer. The temperature of this layer is set to be equal to the local annual average ground ambient temperature [22]. The depth of the top layer can be found with Equation 3 applied to clay. It is determined to be 4.3 meters. The temperature variation at this depth versus time of year for an entire year is shown in Figure 3. The highest temperature throughout the year, at 291 K is taken as the boundary condition to have the worst-case scenario.

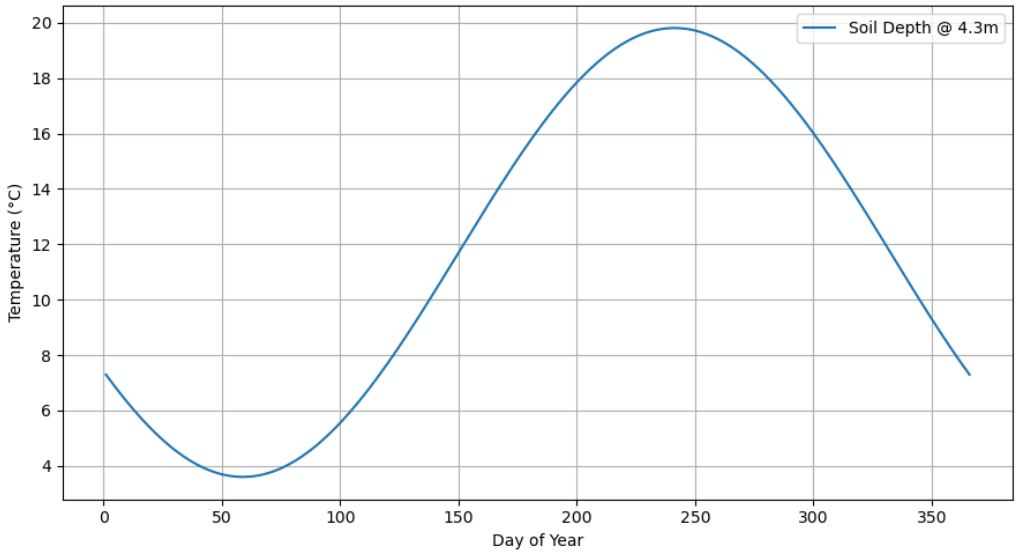

Figure 3: Temperature Distribution of Clay Across a Year

At the reactor vessel, a temperature boundary condition is used for the steady state calculation. For a pool type reactor, two boundary surface conditions are considered. The RPV and the

containment vessel, CV, are considered for this boundary condition. The CV surrounds the RPV, with a gap between the two that is filled with a gas. The placement of PaRRaTS is considered for both CV and RPV boundary conditions. The model temperature boundary condition is an average between the top and bottom values for the RPV and CV. The same height is used, but the radius is different between the two boundary conditions. Table 8 shows the values for these boundary conditions.

Table 8: Reactor Boundary Conditions

Parameter	RPV	CV
Height (m)	17.78	17.78
Diameter (m)	5.74	6.096
Temperature (K)	633	466

2.4 ABAQUS MODEL

ABAQUS 2021 is used to solve the PaRRaTS thermal model. A python script was implemented to loop through all desired model variations allowing the creation of separate models that are then solved and compiled an EXCEL file. This allows for the different case variations to be solved through Idaho National Laboratory's Higher Performance Computing (HPC) system.

The model is composed of four-part instances: inner-shell-1, inner-shell-2, outer-shell with attached-heat-cables, and soil. Conduction interfaces for between the inner-shell-1 and inner-shell-2 components and between the outer-shell-heat-cables component and the soil. A radiation interaction is implemented between inner-shell-2 and the outer-shell. Each part has a separate meshing size and technique, but these values stay constant between the different variations. The inner-shell 2 and outer-shell have finer meshes compared to the inner-shell-1 and soil instances. Three parameters are varied throughout the simulations. These are fin length, fin width, and the number of fins. Ten different values are used for each variable. Only one variable is changed at a time, so the other variable parameters stay constant when one is being varied. Table 9 shows the dimensions that are constant throughout the different simulations. Table 10 shows the different values used for the variables that are changed. All the components have the same height except for the soil.

Table 9: PaRRaTS Constant Dimensions

Dimension	Value
Height (m)	17.78
Inner-shell 1 Thickness (m)	0.1
Inner-shell 2 Thickness (m)	0.2
Fin Length (m)	0.5
Fin Width (m)	0.075
Fin Number	100
Distance between Fin Tip and Outer-shell (m)	0.2
Outer-shell Width (m)	0.5
Heat-cable Length (m)	40
Heat-cable Number	80
Heat-cable Width (m)	0.375
Soil Inner Radius (m)	9
Soil Outer Radius (m)	52.11
Soil Height (m)	30

Table 10: PaRRaTS Variable Dimensions

Dimension	Range
Fin Length (m)	0.5,0.55,0.6,0.65,0.7,0.75,0.8,0.85,0.9,0.95
Fin Width (m)	0.055,0.06,0.065,0.07,0.075,0.08,0.085,0.09,0.095,0.1
Fin Number	40,50,60,70,80,90,100,110,120,130

The model is solved in steady state since normal operating conditions assume no major power fluctuations. The Output Database (ODB) is compiled to get the maximum temperature of the soil, radiative heat flux between the inner-shell-2 and outer-shell and the heat flux between the heat-cables and soil.

To reduce the computational time, a model representing a section of the whole system was solved for instead of one of the entire system. The domain is reduced by taking advantage of cyclic symmetry and by modelling a small section of the height, which is tantamount to assuming perfect insulation at the top and bottom of the system. These simplifications are valid since the system does have cyclic symmetry around the vertical axis of the reactor. A 36-degree model section of the system was solved. A height of 4.445 meters is used. The resulting heat flux is multiplied by 10 and 4 to scale back to a full system. The height section does result in a lower temperature in the soil, but the difference is only a few degrees.

3 RESULTS

Three metrics are used to determine the performance of each modelled system. The maximum temperature of the soil, the radiative heat flux between the inner and outer shells, and the heat flux from the heat-cables into the soil. The heat flux from the heat-cables into the soil is the metric compared to the 0.65 MWt heat removed by the reference RVACS system.

The RPV and CV performances are compared for different fin lengths, widths and numbers. Figure 4 shows the plot of the soil maximum temperature versus different fin lengths. As the fin length increases, the soil temperature increases, which means that PaRRaTS draws more heat from the RPV or the CV as fin length increases. Figure 5 shows the plot of the maximum soil temperature versus different fin widths. A similar, but much less marked, trend is seen, with the temperature rising slightly as the fin width increases. This increase is much lower than observed for the different fin length case. Figure 6 shows the soil's max temperature over different fin numbers. The soil temperature increases with the number of fins. The RPV soil temperature is much higher than the ambient condition, with temperatures over 400 K.

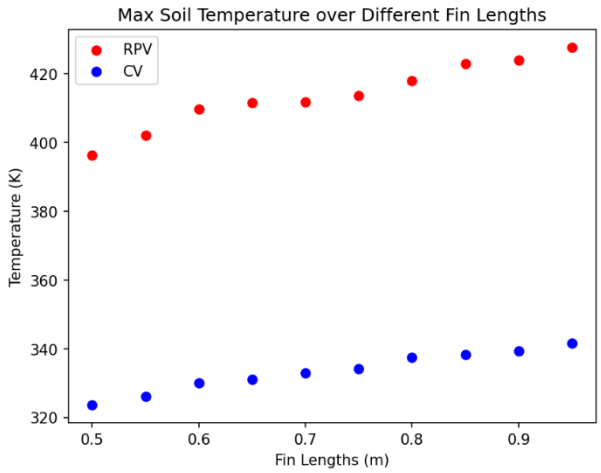

Figure 4: Maximum Soil Temperature versus Fin Lengths

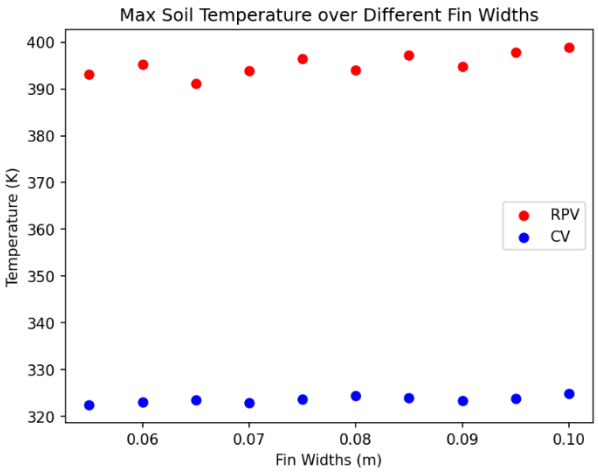

Figure 5: Maximum Soil Temperature versus Fin Widths

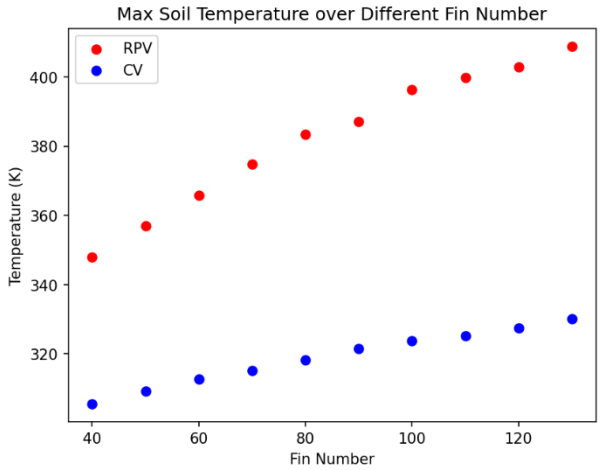

Figure 6: Max Soil Temperature Over Different Fin Numbers

Figure 7 shows the plot of radiative heat transfer between the inner-shell-2 and outer-shell versus fin lengths. The overall observable trend is that radiative heat transfer increases as fin length increases. However, the trend is not fully monotonous with a drop around 0.55 meter and one around 0.85 meter. As of the writing of this preliminary paper, this behaviour still remains under investigation. Figure 8 shows radiative heat transfer for different fin widths for RPV and CV boundary conditions. The heat transfer in the CV case appears essentially independent of fin width. For the RPV boundary condition case, there appears to be an increase as the fin width increases but the trend is not monotonous. This behaviour is still under investigation. Figure 9 shows the radiative heat transfer versus number of fins. Again, the overall trend is an increase versus number of fins, but the behaviour is even more erratic for the RPV and nearly flat for the CV boundary condition case.

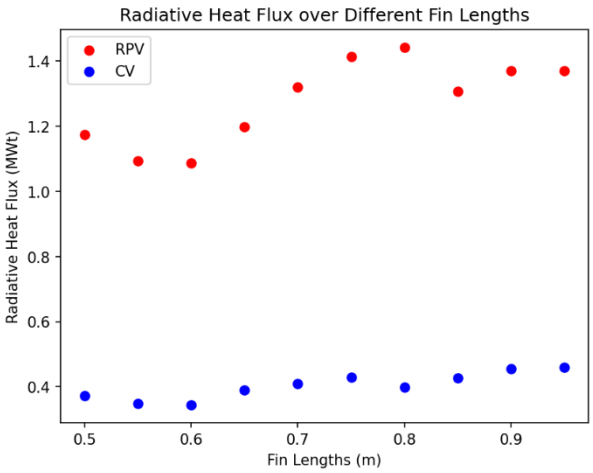

Figure 7: Radiative Heat Flux over Different Fin Lengths

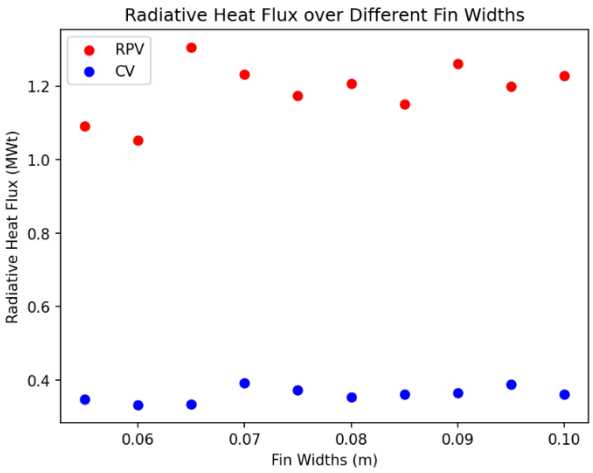

Figure 8: Radiative Heat Flux over Different Fin Widths

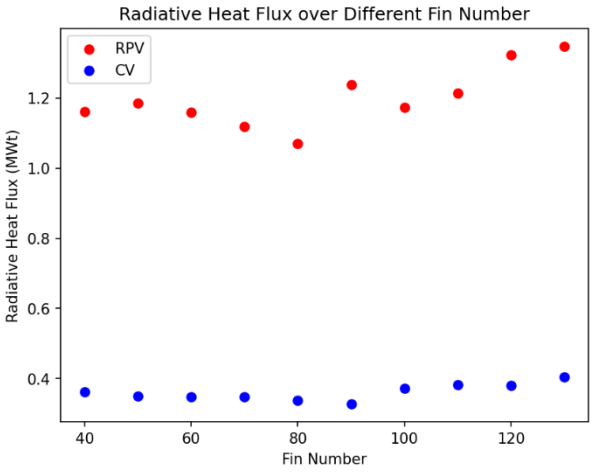

Figure 9: Radiative Heat Flux over Different Fin Numbers

Figure 10 shows the heat flux from the heat cables into the soil versus different fin widths. A similar trend is seen, with the heat flux increasing as fin length increases. In this situation, the trend is much clearer for the CV boundary condition case than for the RPV boundary condition case. Figure 11 shows the heat flux over different fin lengths. The heat flux increases as the fin length increases. Figure 12 shows the heat flux over different fin numbers. The same trend of heat flux increasing with fin number.

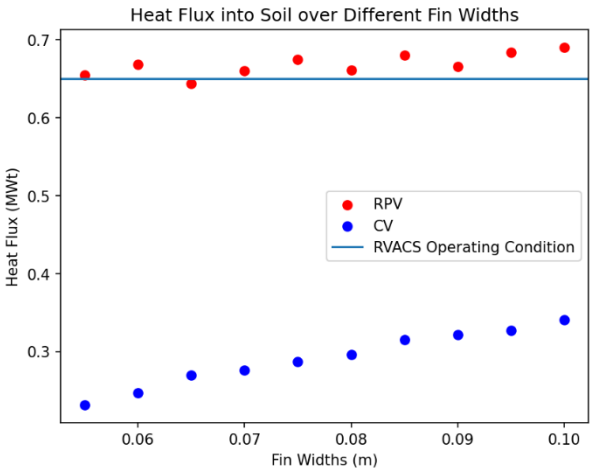

Figure 10: Heat Flux over Different Fin Widths

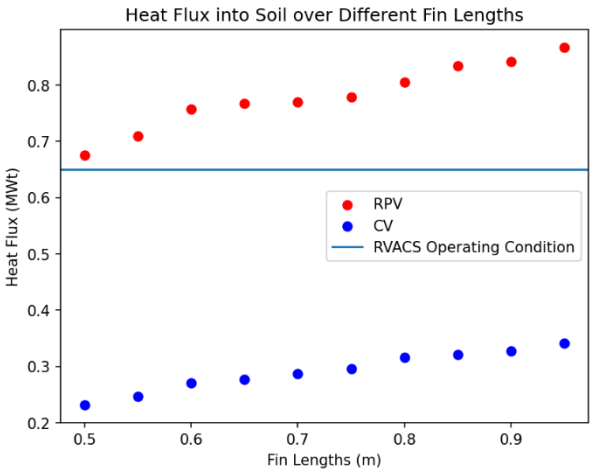

Figure 11: Heat Flux over Different Fin Lengths

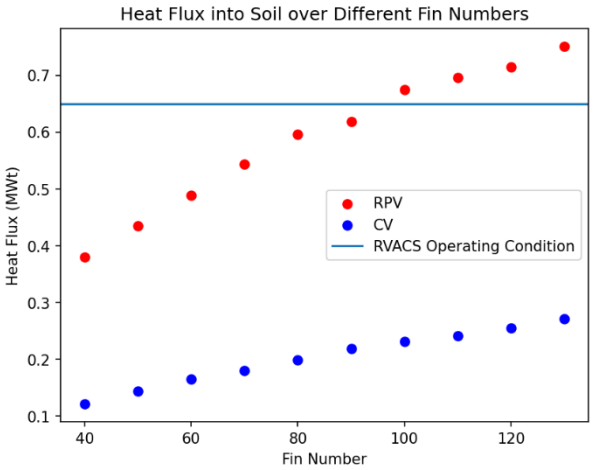

Figure 12: Heat Flux over Different Fin Numbers

4 DISCUSSION AND FUTURE WORK

4.1 Discussion

Radiative heat solutions are erratic, not smoothly behaved. They may require computational refinements that were not possible because of memory and computational resource capacity limitations. Other means to obtain higher fidelity results are under consideration. The conduction results appear reliable and fully meaningful. Work is continuing to reconcile these observations.

For both the RPV and CV boundary condition cases, the performance of the device is highly dependent on its geometry. Increasing the fin length results in a higher surface area between the radiative heat transfer sections. The increase in the number of fins also increases the total surface area. The fin width results in an increase since the distance between the sides of the fins decreases, which alters the view factor and increases the radiative heat transfer while also increasing conduction

within the body of the fins. The increase in the number of fins also changes the view factor with a positive correlation. The fin number has the highest impact on the heat transfer, as seen in the slope of the fin number plots compared to the fin width and length plots.

The soil temperature was shown to increase by 30 to 110 degrees kelvin depending on the modeled design variation. Ideally, the temperature wouldn't increase too much under normal operational conditions. The change in soil temperature would be a concern if the soil temperature were to get too high. This isn't a current concern since the heat cables are to be buried underground so the surface soil should not be significantly impacted.

A difference between the RPV and CV boundary condition cases is also seen. The RPV cases result in higher soil temperatures and heat fluxes compared to the CV cases. This is due to the RPV having a higher operating temperature than the CV. The RPV having a smaller radius than the CV also makes a difference, as the smaller volume results in the heat flux being more concentrated. However, the temperature difference makes a larger difference in this case since the RPV and CV diameters are extremely close.

To compare PaRRaTS performance to the heat loss of the RVACS, the soil heat flux is used. This is used since the output of the system is the heat deposited into the soil. PaRRaTS can be thermally insulating under normal operating conditions, when it removes less heat from the system than an RVACS. The RPV simulation shows more heat removal than RVACS for designs with fin numbers of 100 or higher. This is unideal but there are designs where the RPV conditions show less heat removal than the RVACS.

4.2 Future Work

There are three areas of interest for future work. The effects of parameters that have not been studied, such as shell depths and heat cable properties, will be explored. The shell depths do impact the overall performance, but not as much as the fin parameters do. The heat cables have a lower impact since they will be at lower temperatures than the radiative fins. The second area of interest is the transient performance of PaRRaTS. While it is important for PaRRaTS to insulate during normal operations, what matters most is its ability to handle situations in which no other heat path is available for a shutdown reactor. This is currently being worked on. The third area is optimization of the design. A design that balances insulating during normal operations and heat removal during shutdown conditions is needed. This optimal design should be found through an iterative approach.

5 CONCLUSION

The materials for the PaRRaTS device have been chosen to optimize heat transfer by way of conduction and radiation. It has been found that the PaRRaTS device is insulating during normal operations and that varying the radiative fin geometry impacts the performance of the device. The surrounding soil is heated beyond surface temperature by the device, but the depth and basalt material makes it not a concern. Future work will model PaRRaTS transient behaviour and optimize the geometry for a balance of insulation and heat transmission performance.

6 ACKNOWLEDGEMENTS

This document was authored in part at Idaho National Laboratory (INL) by Battelle Energy Alliance, LLC, under contract no. DE-AC07-05ID14517 with the U.S. Department of Energy (DOE). The work was supported by a NEUP-IRP project. The U.S. Government retains for itself, and others acting on its behalf, a paid-up, nonexclusive, irrevocable, worldwide license in said article to reproduce, prepare derivative works, distribute copies to the public, and perform publicly and display publicly, by or on behalf of the Government. The DOE will provide public access to these results of federally sponsored research in accordance with the DOE Public Access Plan: www.energy.gov/downloads/doe-public-access-plan.

This research made use of Idaho National Laboratory computing resources, which are supported by the Office of Nuclear Energy of the U.S. Department of Energy and the Nuclear Science User Facilities under Contract No. DE-AC07- 05ID1451.

REFERENCES

1. Joanne Liou, "*Safety By Design: How the new generation of nuclear reactors addresses safety,"* IAEA Bulletin, pp.18-19, March 2021, https://www.iaea.org/bulletin/safety-by-design, Accessed: January 18, 2026.

2. Use of Passive Safety Features in Nuclear Power Plant Designs and Their Safety Assessment, IAEA,https://www.iaea.org/topics/design-safety-nuclear-power-plants/passive-safety-features, Accessed: January 18, 2026.

3. D. Lisowski, Q. Lv, B. Alexandreanu, V. Chen, R. Hu, T. Sofu, An Overview of Non-LWR Vessel Cooling Systems for Passive Decay Heat Removal, AL/NSE-21/3, U.S Nuclear Regulatory Commission, Washington, DC, 2021.

4. T. C. Chawla, F. B. Cheung, R. R. Stewart, D. R. Pedersen, J. H. Tessier, R. L. Webb,* H. J. Haupt, T. T. Anderson, E. W. Johanson, C. August, J. R. Pavlik, Modeling of the Air-Side Performance of the RVACS Shutdown Heat Removal System—Status of Experimental Program, ANL-PRISM-8, Argonne National Laboratory, Argonne, IL, 1986

5. PRISM Preliminary Safety Information Document Voume II Chapters 5-8, GEFR-00793, General Electric Advance Nuclear Technology, San Jose, CA, 1987.

6. T. L. Bergman, A. S. Lavine, F. P. Incropera, D. P. Dewitt, Fundamentals of Heat and Mass Transfer, Seventh Edition, John Wiley & Sons, New York, 2011.

7. D. L. Nofziger, J. Wu, Soil Temperature Changes with Time and Depth: Theory, Oklahoma State University, Department of Plant and Soil Sciences, Stillwater, OK, 2003

8. Column Buckling, MechaniCalc, https://www.iaea.org/bulletin/safety-by-design, Accessed: January 19, 2026.

9. ASME, ASME Boiler and Pressure Vessel Code, Section III, Division 1, Subsection NCD, The American Society of Mechanical Engineers, 2023.

10. Daily Metal Prices, Daily Metal Prices, https://www.dailymetalprice.com/, Accessed: June 16, 2025.

11. Hope, How much does Silicon Carbide Cost Per Kilogram, Sanhui, https://sanhuiabrasive.com/faq/how-much-does-silicon-carbide-16,per-kilogram.html#:~:text=Lower-grade%20silicon%20carbide%20for%20abrasive%20purposes%20typically%20costs,and%20semiconductor%20applications%2C%20can%20exceed%20%2420%20per%20kilogram, Accessed: June 16, 2025.

12. CINDAS LLC, Thermophysical Properties of Matter Database, https://cindasdata.com/Applications/TPMD/, Accessed: June 20, 2025.

13. Matmake, Copper Properties, https://matmake.com/materials-data/copper-properties.html, Accessed: June 20, 2025.

14. AZoM, What are the Properties of Aluminum, https://www.azom.com/properties.aspx?ArticleID=1446, Accessed: June 20, 2025.

15. The World Material, 316 Stainless Steel: Properties, Applications, and Data Sheet, https://www.theworldmaterial.com/316-stainless-steel/, Accessed: June 20, 2025.

16. H. Wang, S.K. Vanapalli, A new model for predicting thermal conductivity of unsaturated soils using the soil-water characteristic curve, International Journal of Heat and Mass Transfer, Vol. 247, pp. 127153, 2025.

17. A.M. Ougouag, J.L. Coleman, H. Hiruta, “Part I: Estimating Soil Chemical Composition Relevant to Outdoor Microreactor Deployment at the Critical Infrastructure Test Range Complex,” Idaho National Laboratory draft report 2021.

18. H. Lei, Y. Bo, L. Wang, W. Zhang, Generalized model for predicting the thermal conductivity of fine-grained soils, Geothermics, Vol. 113, pp. 102752, 2023.

19. P. Hartlieb, M. Toifl, F. Kuchar, R. Meisels, T. Antretter, Thermo-physical properties of selected hard rocks and their relation to microwave-assisted comminution, Minerals Engineering, Vol. 91, pp. 34–41, 2016.

20. Ö. Tan, L. Yılmaz, A. Ş. Zaimoğlu, Variation of some engineering properties of clays with heat treatment, Materials Letters, Vol. 58, No. 7, pp. 1176–1179, 2004.
21. J. Han, Q. Sun, H. Xing, Y. Zhang, H. Sun, Experimental study on thermophysical properties of clay after high temperature, Applied Thermal Engineering, Vol. 111, pp. 847–854, 2017.
22. Z. Chen, M. Yu, Y. Mao, K. Zhu, Y. Sun, W. Zhang, P. Cui, Heat transfer model and operation characteristics of borehole heat exchanger with considering geological stratification, ground temperature distribution, atmospheric temperature variation, and upper cover soil layer, Energy and Buildings, Vol. 339, pp. 115775, 2025.